Patterning of fine-features in nanoporous films synthesized by spark ablation

Ji, Xinrui; van Ginkel, Hendrik Joost; Hu, Dong; Schmidt-Ott, Andreas; van Zeijl, Henk; Vollebregt, Sten; Zhang, Guoqi

DOI
10.1109/NANO54668.2022.9928705

Publication date
2022

Document Version
Final published version

Published in
Proceedings of the 2022 IEEE 22nd International Conference on Nanotechnology (NANO)

2022 IEEE 22nd International Conference on Nanotechnology (NANO)
July 4-8, 2022
Palma de Mallorca, Spain

Patterning of fine-features in nanoporous films synthesized by spark ablation

Xinrui Ji†, Hendrik Joost van Ginkel†, Dong Hu, Andreas Schmidt-Ott,
Henk van Zeijl, Sten Vollebregt, Guoqi Zhang

***Abstract*— Advances in semiconductor device manufacturing technologies are enabled by the development and application of novel materials. Especially one class of materials, nanoporous films, became building blocks for a broad range of applications, such as gas sensors and interconnects. Therefore, a versatile fabrication technology is needed to integrate these films and meet the trend towards device miniaturization and high integration density. In this study, we developed a novel method to pattern nanoporous thin films with high flexibility in material selection. Herein, Au and ZnO nanoparticles were synthesized by spark ablation and printed on a Ti/TiO_2 adhesion layer, which was exposed by a lithographic stencil mask. Subsequently, the photoresist was stripped by a cost-efficient lift-off process. Nanoporous patterned features were thus obtained and the finest feature has a gap width of 0.6 μm and a line width of 2 μm. Using SEM and profilometers to investigate the structure of the films, it was demonstrated that the lift-off process had a minor impact on the microstructure and thickness. The samples presented a rough surface and high porosity, indicating a large surface-to-volume ratio. This is supported by the measured conductivity of Au nanoporous film, which is 12% of the value for bulk Au. As lithographic stencil printing is compatible with conventional lithographic pattering, this method enables further application on mass production of various nanoporous film-based devices in the future.**

***Index Terms*— Nanoporous film, Spark ablation, Nanoparticle, Lift-off, Nanofabrication**

I. Introduction

To date, nanoporous materials, as a critical part of nanotechnology, are extensively applied in enormous fields such as gas sensing, catalysis, photochemistry, optoelectronics, and energy storage and conversion. [1]–[3]. Meanwhile, semiconductor devices are rapidly developing towards more functionality and miniaturization [4]. Thus, there is a growing need to integrate functional nanoporous materials and scale down nanoporous patterns.

One typical approach that is often chosen to create nanoporous structures is lithographic patt*Ierning followed by etching and atomic de-alloying [5]–[7]. However, this method is highly materials selective and expensive. Alternatively, printing of nanoporous inks or aerosols is a more flexible and simpler method of obtaining nanoporous structures, but has a limited resolution above 50 μm. To improve the resolution, lithographic patterning can be used. In this regard, lift-off is a simple, low-cost and reliable method to transfer patterns in microfabrication and has been extensively used to pattern bulk materials and thin films [8], [9]. Using lift-off to pattern printed nanoporous thin films is therefore an attractive alternative and could provide a cost-effective and scalable method to apply on such materials. Although some attempts have been made to apply this to nanoporous structures, it is still lacking good control and reproducibility [10].

In the present work, nanoporous structures were fabricated by the lift-off method. The nanoporous film generation is based on nanoparticles synthesis by spark ablation of two opposing electrodes [11], [12]. In contrast to wet chemical synthesis of nanoparticles, no additional chemicals are needed other than the two metallic electrodes and carrier gas. High flexibility in materials selection is also one of its merits and can be achieved by choosing different electrode metals. Spark ablation can be done with pure metals, alloys and some semiconducting materials. To deposit the generated aerosol, an inertial impaction printer, developed by VSPARTICLE B.V., allows contactless, chemical free, maskless and local [13]. The thickness of the nanoporous film and nanoparticle size is tunable with synthesis or printing parameters [11]. Therefore, as a result of combining the strengths of both methods, lift-off of direct-written nanoparticles has a fine resolution, sharp edges, minimal metal waste and enables wafer level printing of complex nanostructured deposits.

In this work, Au and ZnO nanoparticle deposits were patterned using lift-off. The lithographically defined patterns were tested down to a 2 μm resolution. Their microstructure and compatibility to different substrates were investigated and their conductivity was measured.

II. Experimental Section

A. Patterning and lithography

Photolithography was employed to define patterns for wafer-level processing. Fig. 1 shows the fabrication process for the fine nanoporous pattern on a 525 μm p-type Si wafer. At first, a 190 nm low-stress silicon oxide (SiO_2) was deposited by low-pressure-chemical-vapour-deposition (LPCVD). Then, a 25 nm thin Titanium (Ti) layer was sputtered for adhesion. This layer will oxidize fully in ambient air, hence the adhesion layer is TiO_2. Subsequently, a 8.5 μm AZ® 12XT-20PL series photoresist was spin-coated on the surface as shown in Fig. 1(a). A patterned surface structure was then obtained after exposure and development of the photoresist.

Then, the cured photoresist acted as the mask for the lift-off process. As illustrated in Fig. 1(b), a nanoporous film

† Co-first authorship, both authors contributed equally to this publication.

X. Ji, H.J. van Ginkel, D. Hu, S. Vollebregt, H. van Zeijl, G.Q. Zhang are with the Dept. of Electronic Components, Technology and Materials at Delft University of Technology, Mekelweg 4, 2628 CD Delft, Netherlands
A. Schmidt-Ott is with the Faculty of Applied Sciences at Delft University of Technology, Lorentzweg 1, 2628 CJ Delft, Netherlands
Corresponding author: G.Q. Zhang, G.Q.Zhang@tudelft.nl

2022 IEEE 22nd International Conference on Nanotechnology (NANO) | 978-1-6654-5225-0/22/$31.00 ©2022 IEEE | DOI: 10.1109/NANO54668.2022.9928705

was directly written on the surface as described below. After that, the wafers with printed films as shown in Fig. 1(c) were put into a beaker filled with N-Methyl-2-pyrrolidone (NMP) to strip the photoresist in an ultrasonic bath at room temperature for 30 seconds. At the end, the fabrication process was completed by DI water rinse and drying as shown in Fig. 1(d).

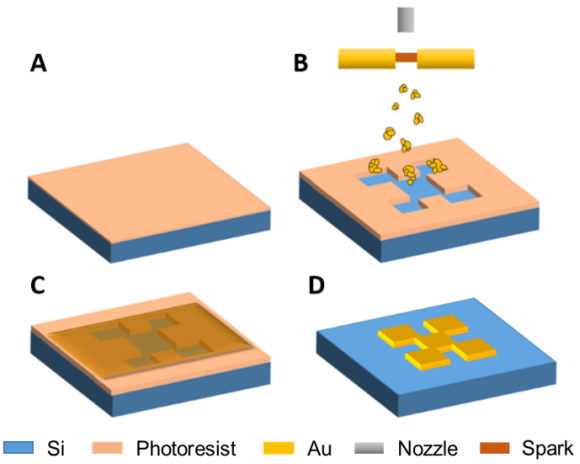

Fig. 1: Fabrication process flow (a) Photoresist coating; (b) Local nanoparticle writing; (c) Synthesized nanoporous film; (d) Patterned nanoporous film.

B. Direct-write setup

Fig. 2 shows a schematic image of our nanomaterial direct-write system with high accuracy and consistency. This system consists of a VSP G1 spark discharge generator and a Proto-0 Nanomaterial Printer that both developed by VSParticle B.V. Pure N_2 (99.999 %) gas was used as carrier gas at a flow rate of 1.5 L/min. Spark conditions were set to 8 mA and 1 kV for Au and 4 mA and 1 kV for ZnO to obtain adequate production rates.

Two opposing electrodes, Au (99.99%) and doped Zn (99.95% Zn 0.05% Al), were ablated to form a nanoparticle aerosol which, after generation, is transported to the printing chamber operating at a <1 mbar vacuum. The pressure difference over the nozzle accelerates the gas and impacts the nanoparticle aerosol onto the substrate. Combining this with a xyz-orientable stage grants the freedom of directly writing nanoporous structures in three dimensions. A nozzle with a flowrate of 0.99 l/min. was adopted in this study. The clean surface of these nanoparticles makes them extremely sensitive to oxidation, and the Zn will oxidize rapidly when exposed to any oxygen to form ZnO [11], [12]. Rectangular patterns were deposited by printing several parallel lines of approximately 1 mm in width with a 0.1 mm spacing, creating an overlap between lines.

C. Material characterization

The microstructure of samples were characterized by a Hitachi Regulus 8230 scanning electron microscope (SEM). A Keyence 3D profilometer was applied to construct 3D profile of the patterned structures. A tip-based Bruker Dektak 150 profilometer was used to determine the thickness and corresponding cross-sectional area of the printed nanoporous lines to compare any changes in the cross-sectional area. The resistance of the patterned structures was measured by a Cascade Microtech probestation with a HP 4156C parameter analyzer.

III. Results and Discussion

A. Microstructure

Fig. 3(a) shows the freshly printed surface of the ZnO nanoporous film on a sequence of rectangular resolution check patterns. Afterwards, the lift-off process was carried out to chemically strip the photoresist as well as the nanoparticle on top of it, leaving only the patterns on the Ti. Fig. 3(b) shows the resulting patterns. It can be seen that the photoresist was washed away, leaving a clean surface without evident contamination. Fig. 3(c) zooms in on the framed area in Fig. 3(b) and the limitation on the resolution was determined to be nearly at the limit of the lithography used to pattern the photoresist. The finest gap being 0.6 µm and the finest film strip being 2 µm. Film strips showed sharp edges. On the edge of the film strips, fences that rolled inward were observed, which were attributed by the nanoparticles stuck on the sidewall of the photoresist pattern. The larger irregularities on the surface were likely caused by extensive nanoparticle aggregation that formed in the printing tubes after synthesis.

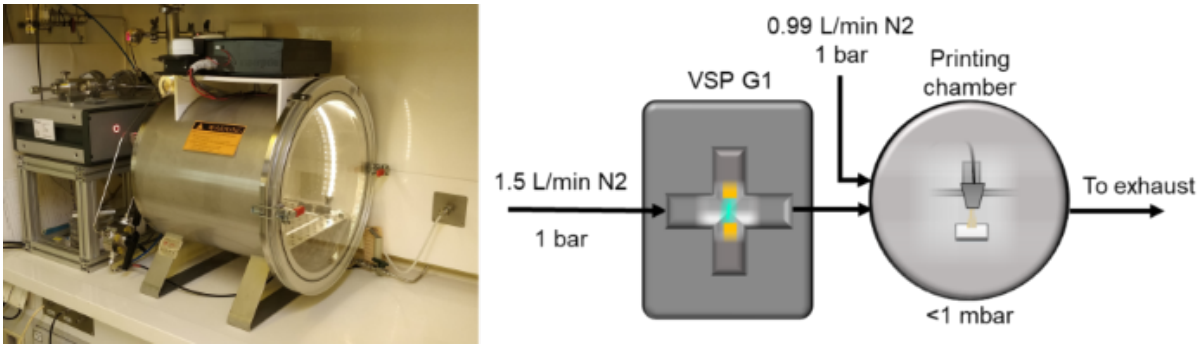

Fig. 2: Photograph of the nanomaterials printer (left) and a schematic diagram showing the major components and gas flow (right)

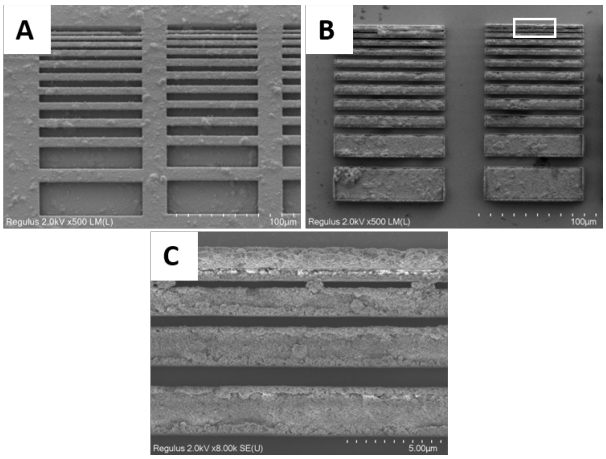

Fig. 3: ZnO sample (a) before lift-off; (b) after lift-off and (c) zoom in.

To study the stability of nanoporous film, the microstructure before and after the lift-off process was studied. First, the change in microstructure was investigated using SEM images as shown in Fig. 4. Before lift-off, it can be seen that the nanoporous film forms a dense, but nanoporous network. The nanoparticles appear to be partially sintered, especially in the case of Au, where there is no oxide boundary to inhibit sintering. The ZnO sample consequently shows a less dense structure. The boundary between individual particles can be recognized in both cases. No clear structural difference is discernible from these SEM images and no organic residue can bee seen, indicating the lift-off process does not affect the nanostructure of the film. As such, the films should retain their original properties derived from their size, which is crucial for their practical application.

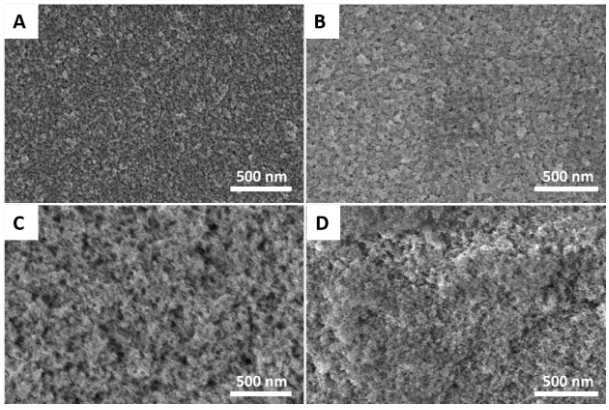

Fig. 4: SEM images showing the microstructure before lift-off (left) and after (right) in Au (top row) and ZnO (bottom row).

Due to the presence of photoresist, the film thickness was impossible to measure without a zero height reference plane. Therefore, a ZnO line was printed onto the Ti/TiO_2 substrate to investigate the influence of the lift-off process on thickness. Six profiles were collected before and after lift-off and averaged to reduce the effect of height differences withing the line. The resulting mean cross-sectional areas from the Dektak measurements are $943 \pm 22\mu m^2$ before and $922 \pm 35\mu m^2$ after lift-off for ZnO and $404 \pm 31\mu m^2$ before and $389 \pm 31\mu m^2$ after for Au. The change after lift of is -2% for ZnO and -4% for Au, which is well within the standard deviations for both before and after measurements. Therefore, we attribute this difference to the limited sample size and small differences in thicknesses along the line. In any case, the difference is minimal, so lift-off does not significantly change the structure.

Van der Pauw structures, as a functional pattern, are shown in Fig. 5. A sharp edge is present in both Au and ZnO nanoporous films. The dark areas in the optical image are attributed to large nanoparticle aggregates, which are big in comparison to the film thickness. This difference is amplified by the 3D image by the stretched z-axis. Such large agglomerated particles, which originate from particle deposition on the tubes of the printer set-up, could be avoided by periodically flushing the system with a fast stream of clean gas. Next, to obtain the average height of the nanoporous film, a hundred lines with an interval of 0.5 µm were measured and averaged, indicated by the red area in Fig. 5. The plotted height information shows a relatively flat surface in both samples. The Au nanoporous film has an average thickness of 1.24 µm while the ZnO one is thicker with 5.31 µm. Zn ablation rates are considerably higher than Au in spark ablation and this is not corrected for in this experiment.

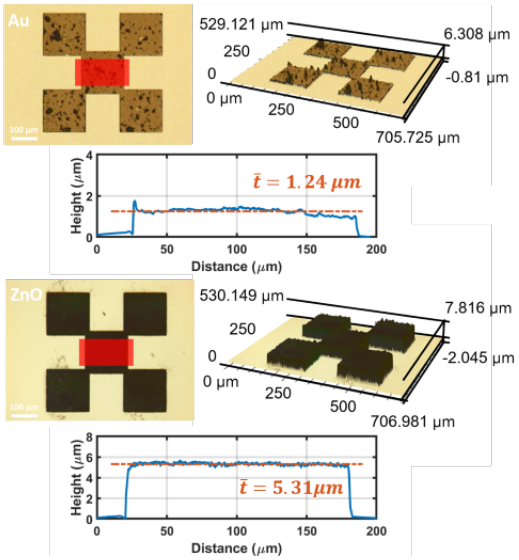

Fig. 5: Van der Pauw structure and height information of and Au Van der Pauw structure (top) and ZnO (bottom). Top view and 3D view of a Van der Pauw structure with corresponding height profile of the red area. The plotted profile is the average of 100 lines, spaced 0.5 µm apart.

B. *Electrical conductivity*

Electrical conductivity is an important property for many applications of these nanoporous films. Patterned square Van der Pauw structures were used in this study to determine the

resistivity of the nanoporous film. Due to the lack of sufficient annealing, ZnO nanoporous film were not conductive, so only the resitivity of Au nanoporous film is presented in this section.

The schematic of measurement is shown in Fig. 6. Voltage was applied on the topside adjacent contacts and the voltage difference and current on the bottom contacts was measured to eliminate contact resistance. A voltage sweep from -0.5V to 0.5V was applied to the Au nanoporous film to induce a current. The I-V curve is plotted in Fig. 6, where good linearity is presented. Afterwards, the resistance was extracted as the inverse of the slope of the linearly fitted line. Subsequently, the resistivity of fabricated nanoporous film was calculated from the Van der Pauw structure by utilizing equation (1) [14].

$$\rho = 4.532 \cdot t \cdot R \tag{1}$$

Where t is the film thickness and R is the resistance measured.

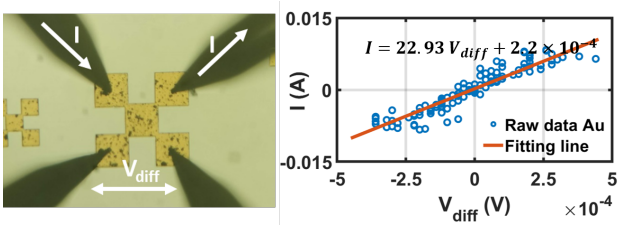

Fig. 6: (a) Schematic of a Van der Pauw measurement and (b) its I-V response.

Combined with the above mentioned thickness as 1.24 µm, the Au nanoporous sample has a resistivity of $2.07 \times 10^{-5}\Omega \cdot \mathrm{cm}^{-1}$. It reaches 8.52 times resistivity of bulk Au ($2.44 \times 10^{-6}\Omega \cdot \mathrm{cm}^{-1}$), which is believed to be mainly caused by its porous structure. Such values enable application in future functional devices. The resistivity of the nanoporous film is related to the degree of sintering and it can be improved by further thermal treatment. Consequently, it can be concluded that our developed nanofabrication process flow is a feasible method to pattern (semi-)conducting nanoporous films with high flexibility in materials selection.

IV. Conclusion

We developed a novel nanofabrication method for fabricating a nanoporous film. Au and ZnO nanoporous films were synthesized by using spark ablation and locally written on Ti/TiO_2 substrate. Subsequently, a lift-off process was applied to pattern nanoporous films. The influence of the wet lift-off process on microstructure and thickness was found to be insignificant. Our fabricated nanoporous film showed the height of 1.24 µm and 5.31 µm for Au and ZnO respectively, with the finest patterned gap width of 0.6 µm and a line width of 2 µm reached in ZnO. We attribute the sharp edges of the resulting structures to a special feature of the impaction printing process applied. As previously shown, impaction printing leads to preferred particle sintering in the vertical direction [12]. Furthermore, the resistivity of the resulting Au nanoporous film was $2.07 \times 10^{-5}\Omega \cdot \mathrm{cm}^{-1}$, which is 8.5 times its bulk state. As a result, we achieved precisely defined Au and ZnO nanoporous film. This work provides a solution for the mass production of nanoporous film-based devices from various materials.

Therefore, using this nanofabrication technology, we can apply such films in integrated devices, while creating a large surface-to-volume ratio on the available area. Since the process flow is compatible with the modern integrated circuit process, it paves the way for effective miniaturization of functional nanoporous patterns.

V. Acknowledgements

This work is supported by NWO grant 729.001.023, Penta Call 3 project SunRISE ref.17004 and Joint Undertaking (JU) under grant agreement No 826417. We also thank the Else Kooi Laboratory and its staff for their technical support in the lab and VSPARTICLE B.V. for the use of their equipment.

References

[1] D. Ji, T. Li, and H. Fuchs, "Patterning and applications of nanoporous structures in organic electronics," Nano Today, vol. 31, p. 100843, 2020.

[2] L. Lu, "Nanoporous noble metal-based alloys: a review on synthesis and applications to electrocatalysis and electrochemical sensing," Microchim. Acta, vol. 186, no. 9, 2019.

[3] G. Q. M. Lu and X. S. Zhao, "Nanoporous materials - an overview," in Nanoporous materials: science and engineering, World Scientific, 2004, pp. 1–14.

[4] G. Q. Zhang, M. Graef, and F. Van Roosmalen, "The rationale and paradigm of 'More than Moore,'" Proc. - Electron. Components Technol. Conf., vol. 2006, pp. 151–157, 2006.

[5] Y. Jiao, J. D. Ryckman, P. N. Ciesielski, C. A. Escobar, G. K. Jennings, and S. M. Weiss, "Patterned nanoporous gold as an effective SERS template," Nanotechnology, vol. 22, no. 29, 2011.

[6] M. M. P. Arnob, F. Zhao, J. Zeng, G. M. Santos, M. Li, and W. C. Shih, "Laser rapid thermal annealing enables tunable plasmonics in nanoporous gold nanoparticles," Nanoscale, vol. 6, no. 21, pp. 12470–12475, 2014.

[7] E. Şeker, W. C. Shih, and K. J. Stine, "Nanoporous metals by alloy corrosion: Bioanalytical and biomedical applications," MRS Bull., vol. 43, no. 1, pp. 49–56, 2018.

[8] G. Klös, A. Andersen, M. Miola, H. Birkedal, and D. S. Sutherland, "Oxidation controlled lift-off of 3D chiral plasmonic Au nano-hooks," Nano Res., vol. 12, no. 7, pp. 1635–1642, 2019.

[9] M. K. Filippidou, M. Chatzichristidi, and S. Chatzandroulis, "A fabrication process of flexible IDE capacitive chemical sensors using a two step lift-off method based on PVA patterning," Sensors Actuators, B Chem., vol. 284, no. June 2018, pp. 7–12, 2019.

[10] B. Zhang, Y. C. P. Carisey, A. Damian, R. H. Poelma, G. Q. Zhang, and H. W. van Zeijl, "3D interconnect technology based on low temperature copper nanoparticle sintering," in 2016 17th International Conference on Electronic Packaging Technology (ICEPT), Aug. 2016, pp. 1163–1167.

[11] Andreas Schmidt-Ott, Spark Ablation: Building Blocks for Nanotechnology. CRC Press, 2019.

[12] T. Pfeiffer, J. Feng, and A. Schmidt-Ott, "New developments in spark production of nanoparticles,"Advanced Powder Technology,vol. 25, no. 1, pp. 56–70, 2014.

[13] H. J. van Ginkel, J. Romijn, S. Vollebregt, and G. Q. Zhang, "High Step Coverage Interconnects By Printed Nanoparticles," in European Microelectronics and Packaging Conference and Exhibition (EMPC), 2021, pp. 1–4.

[14] M. J. Deen and F. Pascal, "Electrical characterization of semiconductor materials and devices - Review," J. Mater. Sci. Mater. Electron., vol. 17, no. 8, pp. 549–575, 2006.